

Infrared observation of femtosecond laser inscribed gratings

Andreas Ioannou,^{1,2,*} Antreas Theodosiou,² Kyriacos Kalli,² and Christophe Caucheteur,¹

¹Electromagnetism and Telecommunication Department, University of Mons, Boulevard Dolez 31, 7000 Mons, Belgium

²Photonics & Optical Sensors Research Laboratory (PhOSLab), Cyprus University of Technology, 31 Archbishop Kyprianos Street, 3036 Limassol, Cyprus

Abstract

In this work, TFBGs were inscribed in single mode optical fiber using the direct writing plane-by-plane femtosecond-laser inscription method. This new technique presents a unique characteristic; it enables the excitation of higher order cladding modes. An infrared camera observation system was built to examine the behavior of these cladding modes, across the surface of the fiber. Then, a tunable laser was used to scan the 1520-1610 nm wavelength range and the intensity profile of the corresponding modes was captured. From our observations, radiation happens at specific wavelengths that closely match the cladding mode resonances of the transmission spectrum.

Femtosecond laser inscription

TFBGs were inscribed in FiberCore photosensitive single-mode optical fiber using the plane-by-plane femtosecond laser inscription method [1]; a flexible approach offering control of the grating period, and the length, width and depth of the grating planes. Fiber samples were mounted on highly accurate air-bearing translation stages (Aerotech) allowing for controlled movement during the inscription procedure. 220 fs pulses generated at 517 nm by a femtosecond laser HighQ laser femtoREGEN were focused through a long working distance objective (Mitutoyo x50) to the fiber core using a third translation stage. Grating planes were produced with a width of ~ 800 nm, following the process described in [2]. Figure 1 displays a microscope image of the grating produced in the fiber core. Its actual period is $4.366 \mu\text{m}$, so that the 8th order grating can be in the wavelength range [1500-1580 nm], as shown in Figure 2.

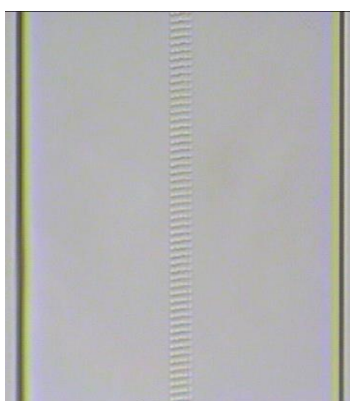


Fig. 1 Microscope image of a 8th order 7° TFBG in $8.2 \mu\text{m}$ fiber core.

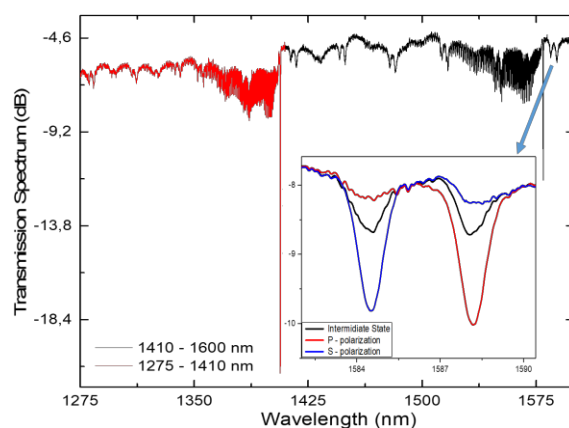


Fig. 2 Transmitted spectrum of a 8th order 7° TFBG in the wavelength range 1410-1600 nm (black) and 1275-1410 nm (red). Inset: Polarization dependence of ultra-high order cladding mode.

The energy of pulses at the output of the laser was measured as 100 nJ per pulse, and with a repetition rate of 50 kHz. The jacket of the fiber was not removed for the inscription process, thus retaining the fiber's integrity throughout the irradiation.

Experimental observation setup

Figure 3 displays the infrared camera observation system. A three-lens magnification setup was implemented along with an x10 microscope objective and manual fiber rotators were placed over the controlled z-stage for adequate observation of the fiber surface in all angles.

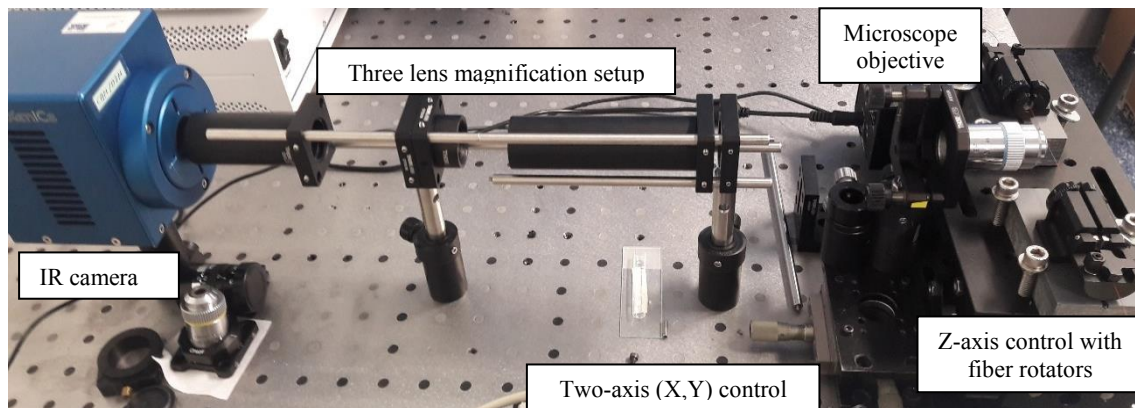


Fig. 3 Infrared camera observation setup.

A tunable laser Exfo FLS-2600B was used to scan the spectrum in the range [1520-1610 nm] to analyze the scattered intensity in a 2-scan process. The initial scan took place in order to initialize the software parameters of the IR camera (XenICs – Xena 435) capturing software. The camera can measure the pixel intensity it captures. In that way, we made sure that the radiation intensity never saturated the camera, thus making sure that our observations reflect well the behavior of the different modes, as depicted in Figure 4.

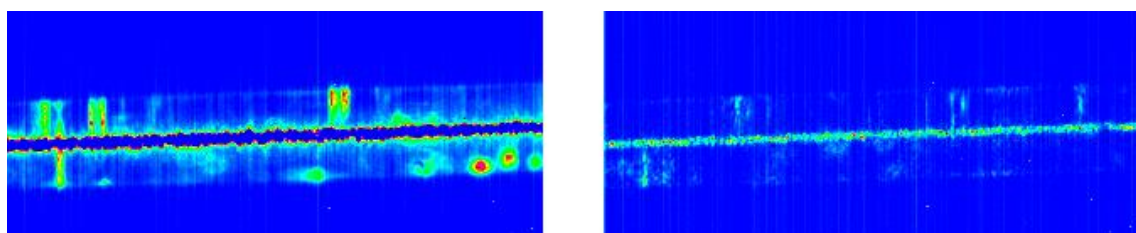


Fig. 4 Transverse radiation of the 8th order 7° TFBG captured with the camera: with a 10 mW white light source as an input, featuring saturation of the camera (left), and with a 1 mW tunable laser source, displaying a correct image (right).

The fiber was stripped in order to observe the scattering. At this point the higher order cladding modes appeared in the transmission spectrum. We measured the evolution of the intensity, as we scanned the wavelength spectrum with the tunable laser source. Figure 5 shows the dependence on direction for 4 different positions set with the manual rotators. As expected, the camera records a higher light intensity for the fiber orientation corresponding to the perpendicular of the tilted grating planes.

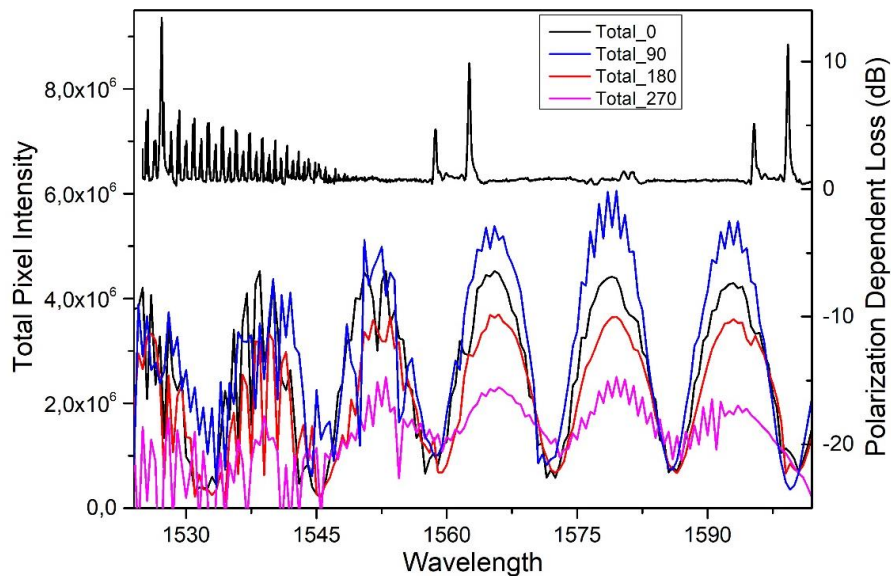


Fig. 5 Total pixel intensity measured by the infrared camera for four orthogonal directions of the fiber for an 8th order 7° TFBG.

As shown in our previous work [3], higher order cladding modes can be more easily distinguished in the PDL (polarization dependent loss) curve. The latter is also presented in Figure 5, to identify the location of the higher order cladding modes in the spectrum. It is obvious that some modes captured by the observation system are absent from the PDL spectrum. We attribute this observation to two main reasons. First, cladding modes originate from multiple higher grating orders. Some of them are not strong enough to intermingle in the observable spectrum but they leak out nevertheless [4]. Secondly, the wavelength position and strength of all cladding modes (from all grating orders) in the transmitted spectrum is closely related to the surrounding refractive index value [5]. To reflect this dependence, we have coated the sample with a thin layer of gold (~50nm), like in the case of surface plasmon resonance (SPR) based sensors [6]. Figures 6 and 7 show the transmission spectrum and the PDL of a grating before and after gold deposition. The distribution of higher order cladding modes clearly changed. Some higher order cladding modes are enhanced while other are decreased, reflecting well that the surrounding medium strongly influences them.

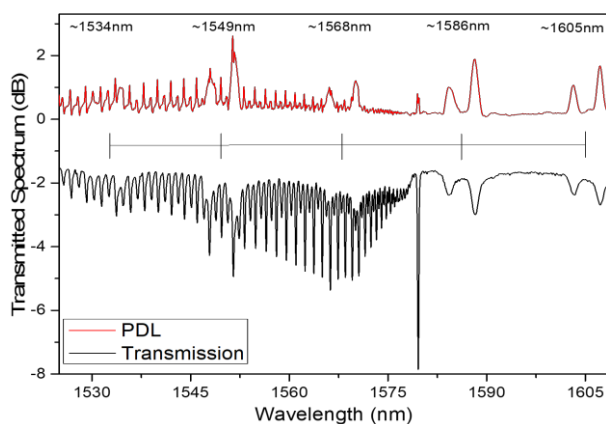


Fig. 6 Transmission spectra (black) and PDL (red) of the grating under study, where we visualize the higher order cladding modes.

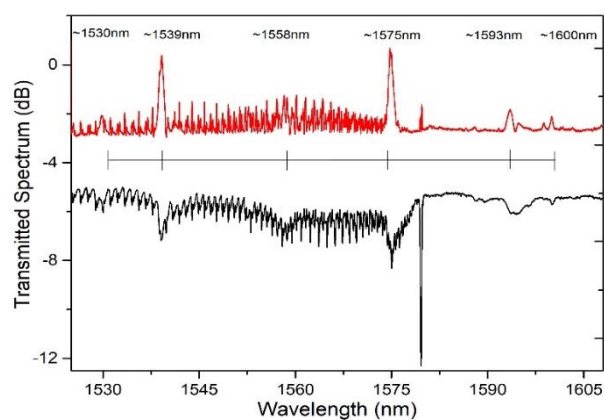


Fig. 7 Transmission spectra (black) and PDL (red) of the same TFBG after the 50 nm of Au coating.

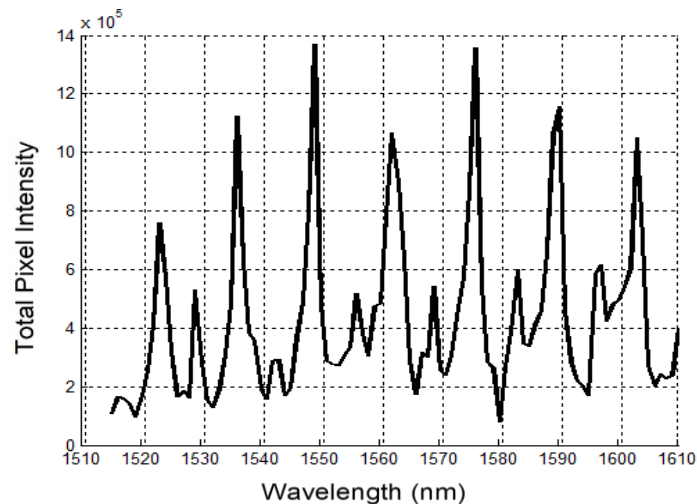


Fig. 8 Higher order cladding mode observation on the transverse surface of the fiber of the coated TFBG.

This is also reflected in figure 8 that presents the higher order cladding mode evolution across the spectrum. We observe that the acquired intensity profile is a composite of all the interfering modes, even if those modes do not appear in the transmission spectrum or PDL.

Conclusions

In this work, we have presented the ability to visualize the appearance of higher order cladding modes; a product of the femtosecond laser PI-by-PI inscription process. We plan to further examine the possibilities of this unique characteristic and find possible opportunities to implement, also for particle manipulation.

Authors acknowledge the financial support of the F.R.S.-FNRS (PDR project PSOFT, EOS project CHARMING and Associate Research grant of C. Caucheteur).

References

- [1] A. Theodosiou, A. Lacraz, A. Stassis, C. Koutsides, M. Komodromos, and K. Kalli, "Plane-by-Plane Femtosecond Laser Inscription Method for Single-Peak Bragg Gratings in Multimode CYTOP Polymer Optical Fiber," *J. Light. Technol.*, vol. 35, no. 24, pp. 5404–5410, 2017.
- [2] A. Ioannou, A. Theodosiou, C. Caucheteur, and K. Kalli, "Direct writing of plane-by-plane tilted fiber Bragg gratings using a femtosecond laser," *Opt. Lett.*, vol. 42, no. 24, p. 5198, 2017.
- [3] A. Ioannou, A. Theodosiou, K. Kalli, and C. Caucheteur, "Higher-order cladding mode excitation of femtosecond-laser-inscribed tilted FBGs," *Opt. Lett.*, vol. 43, no. 9, p. 2169, 2018.
- [4] A. W. Snyder and D. J. Mitchell, "Leaky mode analysis of circular optical waveguides," *Opto-electronics*, vol. 6, no. 4, pp. 287–296, 1974.
- [5] G. Laffon and P. Ferdinand, "Tilted short-period fibre-Bragg-grating-induced coupling to cladding modes for accurate refractometry," *Meas. Sci. Technol.*, vol. 12, no. 7, pp. 765–770, 2001.
- [6] C. Caucheteur, T. Guo, and J. Albert, "Polarization-Assisted Fiber Bragg Grating Sensors: Tutorial and Review," *J. Light. Technol.*, vol. 35, no. 16, pp. 3311–3322, 2017.